Nuclear Physics B154 (1979) 173–188

CALCULATION OF CRITICAL POMERON INTERCEPT WITH BLOCK-SPIN METHODS

R. DEZA and L. MASPERI
*Centro Atómico Bariloche *, Instituto Balseiro **, 8400 S.C. de Bariloche, R.N. Argentina*

Received 8 March 1979

The single-site energy eigenvalues and field matrix elements of reggeon field theory are accurately calculated. Using the block-spin approximation with realistic parameters, the phase transition is studied in one and two dimensions using different methods. In one dimension, the use of blocks with one site and one link gives a critical temperature in agreement with that predicted by the high-temperature expansion. In two dimensions, the methods with critical temperature around the high-temperature expansion result, give a critical pomeron intercept larger than 1.05 in the physical range.

1. Introduction

The phase transition which occurs in reggeon field theory [1] (RFT) has been studied in several papers. Most of them [2–5] take its lattice version and build the single-site Hamiltonian and intersite interaction using expressions valid for the bare pomeron intercept $\alpha_0 \gg 1$, or, alternatively, for the bare slope α' and triple coupling r_0 very small. In this way the general features of the phase transition were obtained.

Since the phenomenological applications of RFT [6] are based on the knowledge of the value of the critical intercept of the bare pomeron, α_c, it is interesting to calculate this number accurately. Its evaluation depends on the lattice spacing b, related to the experimental momentum-transfer cutoff of the triple-pomeron coupling, and on the actual values of α' and r_0. An attempt was then made [7] to start from a more realistic lattice Hamiltonian using single-site eigenvectors obtained from those [8] corresponding to $\alpha_0 < 1$ through a variational procedure. Though it was thus possible to calculate the intercept renormalization in the subcritical region $\alpha_0 < \alpha_c$ using the block-spin method of 2-site cells in two dimensions of ref. [3], the phase transition could not be reached for the most realistic values of b due to the breakdown of the approximation for the single-site states. Therefore, the value of α_c could only be estimated by an extrapolation.

* Comisión Nacional de Energía Atómica.
** Universidad Nacional de Cuyo.

The purpose of the present work is to evaluate α_c with greater accuracy. For this one must first calculate the realistic single-site matrices, and then test different block-spin procedures for taking the intersite interaction into account.

We were able to solve the single-site problem numerically, expanding the eigenfunctions in power series and demanding the known asymptotic behaviour. The first and second excited eigenvalues and the matrix elements of the field in the subspace of the two lowest states turn out to agree with the perturbative values for $\alpha_0 \ll 1$ and with the asymptotic expressions used in refs. [2–5] for $\alpha_0 \gg 1$.

Regarding the intersite problem, we have compared different block-spin procedures. For $D = 1$ transverse dimension it turns out that while the two-site cell method of ref. [3] gives too high a critical temperature compared to the result of the high-temperature expansion [4], the latter is perfectly reproduced by the trick of omitting one of the site contributions [9]. In $D = 2$ dimensions we have tried two-site cell procedures, omitting or not omitting one site contribution, and four-site cells, again excluding or not excluding one site term [10]. The critical temperature obtained with the high-temperature expansion hes between the results of the last two methods. Finally, we have looked at the influence of leaving the direct terms arising from the approximation of the gradient as an intersite interaction. This produces a very slight variation of the value of α_c. The critical intercept obtained with the more reasonable methods is $\alpha_c \geqslant 1.05$, a value slightly higher than previous estimates [7].

In sect. 2 we describe the numerical solution of the single-site problem and give the results for the eigenvalues and matrix elements. In sect. 3 we analyze the different block-spin calculations and we end with a few conclusions in sect. 4.

2. Single-site energy eigenvalues and field matrix elements

The single-site Hamiltonian of the RFT is

$$H_1 = \tilde{\Delta}\bar{\psi}\psi + i\tfrac{1}{2}\tilde{r}\bar{\psi}(\psi + \bar{\psi})\psi , \tag{1}$$

where $\Delta_0 = 1 - \alpha_0$, $\tilde{\Delta} = \Delta_0 + 2D\alpha'/b^2$ and $\tilde{r} = r_0/b^{D/2}$. In the above expression we have included the term $(2D\alpha'/b^2)\bar{\psi}\psi$ which comes from the direct contribution produced by the approximation $\nabla\psi = (\psi_{j+1} - \psi_j)/b$. It is also possible to leave this term among the intersite interactions.

Using Bargmann's representation [11]

$$\phi_n(z) = \langle 0|e^{az}|n\rangle , \qquad \psi = a \to \frac{\mathrm{d}}{\mathrm{d}z} , \qquad \bar{\psi} = a^+ \to z , \tag{2}$$

where $a(a^+)$ is the annihilation (creation) operator and z is a complex variable, the eigenvalue equation $H_1|n\rangle = E_n|n\rangle$ can be written as

$$z\left[\rho + i\left(z + \frac{\mathrm{d}}{\mathrm{d}z}\right)\right]\frac{\mathrm{d}}{\mathrm{d}z}\phi_n(z) = \lambda_n\phi_n(z) , \tag{3}$$

where we have introduced the relevant parameter $\rho = 2\tilde{\Delta}/\tilde{r}$ and expressed the eigenvalues as $\lambda_n = 2E_n/\tilde{r}$.

To have normalizable states ϕ_n according to

$$\langle \phi_n, \phi_n \rangle = \int \frac{dz dz^*}{2\pi i} e^{-zz^*} |\phi_n(z)|^2 < \infty , \tag{4}$$

it is necessary that

$$\phi_n(z) \xrightarrow[z \to -i\infty]{} \text{constant} . \tag{5}$$

The condition on the negative imaginary axis eq. (5) allows us to find the energy eigenvalues. In fact, apart from the vacuum $\lambda_0 = 0$ corresponding to $\phi_0 = \text{constant}$, the only possible expansion of ϕ_n is

$$\phi_n(z) = z \sum_{m=0}^{\infty} c_m z^m , \tag{6}$$

with the recursion relation

$$c_{m+1} = \frac{-m c_{m-1} + i[(m+1)\rho - \lambda_n] c_m}{(m+2)(m+1)} , \tag{7}$$

which can be derived from eq. (3). Given a value for ρ, the corresponding eigenvalues λ_n are obtained as those which through eqs. (7), (6) produce the asymptotic behaviour of eq. (5).

To apply the spin approximation of RFT we need the matrix elements of ψ and $\bar{\psi}$ in the subspace of the vacuum and first excited state. Normalizing the state ϕ_1 according to

$$\int \frac{dz dz^*}{2\pi i} e^{-zz^*} \phi_1(z^*) \phi_1(z) = 1 , \tag{8}$$

since the left eigenvector [11] is $\phi_1^*(z^*)$, these matrix elements can be evaluated by means of

$$\langle 1|\psi|1\rangle = \langle 1|\bar{\psi}|1\rangle = \int \frac{dz dz^*}{2\pi i} e^{-zz^*} \phi_1(z^*) z \phi_1(z) , \tag{9}$$

and

$$\langle 1|\bar{\psi}|0\rangle = \langle 0|\psi|1\rangle = \left. \frac{d\phi_1(z)}{dz} \right|_{z=0} = c_0 . \tag{10}$$

If we leave the direct term coming from the gradient product among the intersite interactions, it will also be necessary to compute the matrix element

$$\langle 1|\bar{\psi}\psi|1\rangle = \int \frac{dz dz^*}{2\pi i} e^{-zz^*} \phi_1(z^*) z \frac{d}{dz} \phi_1(z) . \tag{11}$$

Table 1
Single-site results

ρ	λ_1	$\langle 0\|\psi\|1\rangle$	$i\langle 1\|\bar{\psi}\|1\rangle$	$\langle 1\|\bar{\psi}\psi\|1\rangle$
5	5.3522885457	1.030	0.343	0.944
3	3.50717910	1.060	0.484	0.894
2	2.6354151	1.092	0.595	0.846
1	1.824763	1.149	0.753	0.769
0.5	1.45299	1.194	0.856	0.716
0	1.11128	1.257	0.982	0.649
−0.5	0.8065	1.35	1.13	0.568
−1	0.5462	1.47	1.32	0.471
−2.5	0.084	2.24	2.22	0.149
−5	$\sim 10^{-4}$	4.8	4.8	$\sim 10^{-2}$

First-excited level $\lambda_1 = 2E_1\sqrt{r}$ and matrix elements calculated with eqs. (9)–(11) are shown for different values of $\rho = 2\tilde{\Delta}/r$.

We have calculated 100 coefficients of eq. (6) observing that the corresponding series $\phi_n(z)$ tend to a constant for z on the negative imaginary axis up to $|z| = 4$ when the values of λ_n are those shown in table 1 and fig. 1a. The upper limit on the number of coefficients is given by their smallness for $m > 100$. Changing the

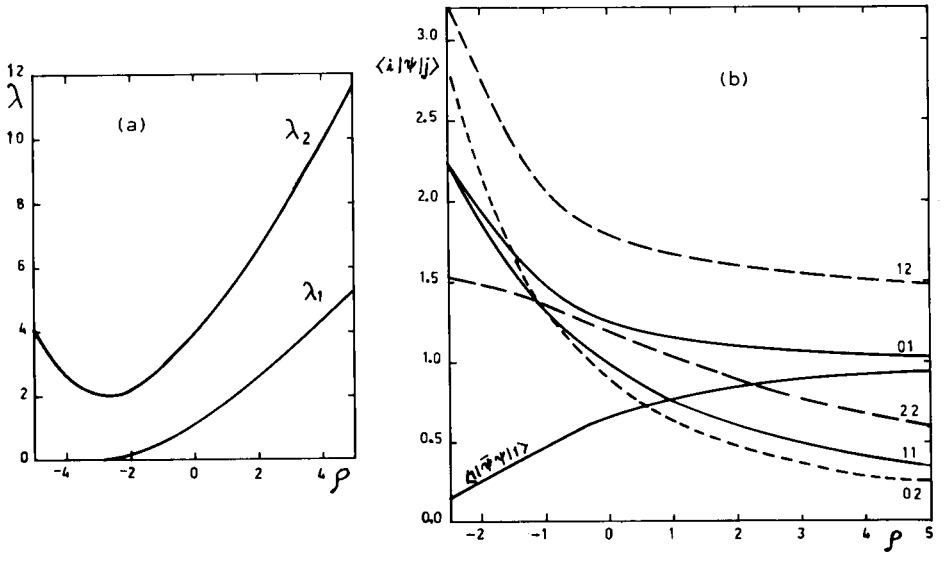

Fig. 1. (a) First and second excited levels of the single-site Hamiltonian, eq. (3). (b) Field matrix elements between vacuum, first and second excited single-site states, eqs. (9)–(11).

values of λ_1 by one unit of the last significant figure of table 1, the resulting series shows a divergent behaviour for $iz < 4$. On the other hand the stability of our results is given by the following examples. For $\rho = 5$ and keeping only 20 terms in the series, all 11 significant figures of λ_1 do not change. For $\rho = -1$ the stability is smaller, since one needs at least 55 terms of the series to reproduce the 4 significant figures shown in table 1. With the function ϕ_1 so defined, we have performed the integrals eqs. (8), (9), (11), obtaining the matrix elements shown in table 1 and fig. 1b. The upper limit of the complex integrals was $|z| = 4$ and the significant figures given in table 1 remain constant if this upper limit is decreased to $|z| = 3$.

Regarding the values around $\rho = -5$, which correspond to the very supercritical region, we see that the order of magnitude of λ_1 agrees with the exponential formula

$$\lambda_1 \approx \frac{1}{\sqrt{2\pi}} \rho^2 \exp(-\tfrac{1}{2}\rho^2) ,$$

and that

$$|\langle 0|\psi|1\rangle| \simeq |\langle 1|\bar{\psi}|1\rangle| \approx |\rho| ,$$

as expected [2]. In this region λ_2 is still smaller than the limiting value $|\rho|$, though not so small as the value estimated by the semiquantum method [12]. Though accurate, our calculations in the very supercritical region are not as precise as those for $\rho \gtrsim 0$ because the coefficient c_m decrease faster for small $\rho - \lambda_1$.

In the very subcritical region, $\rho \simeq 5$, our results can be compared with the perturbative ones which, taking as the perturbation the Hamiltonian $ia^+(a + a^+)\, a$ (see eq. (1)), are

$$\lambda_1^{(2)} = \rho + \frac{2}{\rho}, \qquad \lambda_2^{(2)} = 2\rho + \frac{10}{\rho}, \tag{12}$$

as second-order energies, and

$$\begin{aligned} &\langle 0|\psi|1\rangle = 1 , \quad \langle 1|\bar{\psi}|1\rangle = -i2/\rho , \quad \langle 0|\psi|2\rangle = i\sqrt{2}/\rho , \\ &\langle 1|\psi|2\rangle = \sqrt{2} , \quad \langle 2|\bar{\psi}|2\rangle = -i4/\rho , \quad \langle 1|\bar{\psi}|2\rangle = 0 , \end{aligned} \tag{13}$$

as first-order matrix elements. We can see from table 2 that this comparison is satisfactory and at the same time that the agreement with the semiquantum results in this region [12] is good.

For $\rho > 0$ and not too high the present results for λ_1 and for the matrix elements are in fair agreement with the less accurate values obtained in ref. [7].

From fig. 1a it can be seen that in the region $\rho \sim 0$ which, as will be seen in sect. 3, corresponds to the critical zone, $\lambda_1 - \lambda_0 < \lambda_2 - \lambda_1$. In addition, from table 1 and for all the analyzed region of ρ, it is verified that

$$\langle 1|\bar{\psi}\psi|1\rangle \approx |\langle 0|\psi|1\rangle|^2 - |\langle 1|\bar{\psi}|1\rangle|^2 ,$$

Table 2
Comparison with perturbation and semiquantum approximations

$\rho = 5$	Present calculation	Perturbation	Semiquantum
λ_1	5.3522885457	5.4	5.3
λ_2	11.618395987	12.	11.4
$\langle 0\|\psi\|1\rangle$	1.030	1.0	
$i\langle 1\|\bar{\psi}\|1\rangle$	0.343	0.40	0.35
$-i\langle 0\|\psi\|2\rangle$	0.255	0.28	
$i\langle 2\|\bar{\psi}\|2\rangle$	0.60	0.80	0.54
$\langle 1\|\psi\|2\rangle$	1.48	1.41	
$\langle 1\|\bar{\psi}\|2\rangle$	0.03	0	

First and second excited levels and field matrix elements between them and vacuum are compared with second-order perturbative results, eqs. (12) and (13), and with the semiquantum method based on ref. [12].

showing that the matrix elements $\langle 1|\bar{\psi}|n\rangle$ with $n > 1$ are small. However, from fig. 1b one sees that the couplings between the states $|0\rangle$ and $|2\rangle$, and $|1\rangle$ and $|2\rangle$ given by $\langle 0|\psi|2\rangle$ and $\langle 1|\psi|2\rangle$ are sizeable and increase for negative ρ.

Performing the non-unitary transformation

$$\phi(x) = (x^2)^{1/4} \exp[\tfrac{1}{4}(x^2 + \rho)^2]\ \hat{\phi}(x)\,, \tag{14}$$

where $z = -ix^2$, the eigenvalue equation, (3), takes the familiar Schrödinger form

$$\left\{-\tfrac{1}{2}\frac{d^2}{dx^2} + \tfrac{3}{8}\frac{1}{x^2} + \frac{x^2}{2}[(x^2 + \rho)^2 - 2]\right\} \hat{\phi}_n(x) = 2\lambda_n \hat{\phi}_n(x)\,. \tag{15}$$

This equation has been analyzed by the semiquantum method in ref. [12] and with greater accuracy here, giving the results shown in table 2. The ground state of eq. (15), which corresponds to the first excited level λ_1 has been also analyzed by a variational method based on the assumption of a $\hat{\phi}$ which has the correct behaviour for $x \to 0$ and $x \to \infty$ and is centered around the minimum of the potential. Note that for $\rho \lesssim -3$ this potential develops a second minimum but the ground state is still centered around the deepest well. The energy eigenvalues are in agreement with those of table 1, e.g., for $\rho = 1$ this variational method gave $\lambda_1 = 1.87$.

3. Block-spin calculations

To implement a tractable renormalization group procedure for RFT on the lattice we shall keep only the two lowest levels in each site even though for $\rho \sim 0$, which will correspond to the critical region, the second excited state is not too far from the first and the coupling between them is not weak. It has been shown in ref. [7] that, keeping three levels for the first step in the block-spin calculation, the two

lowest levels of the cells are not very much affected. On the other hand, to keep three levels systematically would imply handling too many parameters (the 3 × 3 matrix for ψ contains 5 non-zero elements as shown in fig. 1b); it is clear that the two-level approximation is one of the main sources of error in the calculation of the critical intercept.

Having decided to keep only two levels per site, one must determine whether all the term $\alpha' \nabla\bar{\psi} \cdot \nabla\psi$ will be taken as the intersite interaction or only the non-diagonal part of its lattice version. We shall consider the latter possibility, which is the usual choice, in subsect. 3.1 and the former alternative in subsect. 3.2.

3.1. *Inclusion of the diagonal part of* $\nabla\bar{\psi} \cdot \nabla\psi$ *in the single-site Hamiltonian*

The Hamiltonian for RFT on the lattice is

$$H = \sum_j \left\{ \begin{pmatrix} 0 & 0 \\ 0 & \epsilon \end{pmatrix}_j - K \sum_{\hat{\imath}} \left[\begin{pmatrix} 0 & 0 \\ 0 & i\tau \end{pmatrix}_j \begin{pmatrix} 0 & 1 \\ 0 & i\tau \end{pmatrix}_{j+\hat{\imath}} + \begin{pmatrix} 0 & 1 \\ 0 & i\tau \end{pmatrix}_j \begin{pmatrix} 0 & 0 \\ 1 & i\tau \end{pmatrix}_{j+\hat{\imath}} \right] \right\}, \tag{16}$$

where

$$\epsilon = E_1 , \qquad K = \frac{\alpha'}{b^2} (\langle 0|\psi|1\rangle)^2 , \quad i\tau = \frac{\langle 1|\bar{\psi}|1\rangle}{\langle 0|\psi|1\rangle},$$

and $\hat{\imath}$ denotes the nearest neighbours to site j along the positive orientation of the spatial axis.

We shall consider the simplest $D = 1$ case and then the realistic $D = 2$ situation.

3.1.1. $D = 1$.

As usual, we shall take two-site cells. The block-spin calculation including the energy of both sites and the link term in the block Hamiltonian has been performed in ref. [3] giving the critical relation $T_c = \epsilon/K = 1.15$ for $|\tau| = 1$. If $\epsilon/K > T_c$, one is in the disordered phase and $\epsilon \to$ finite, $K \to 0$, while $\epsilon/K < T_c$ corresponds to the ordered phase and $\epsilon \to 0$, $K \to$ finite.

It has been shown in ref. [9] that for the Ising model with transverse field in one dimension the correct critical ratio of parameters is obtained by including only one energy site and one link in the block Hamiltonian. This procedure has the virtue of maintaining for the block the self-duality [13] property of the chain.

In RFT it is not apparent that any self-duality symmetry holds. However, the method of ref. [9] can also be tested in this case, having at least the property of taking for the block the same proportion of sites and links as in the whole chain. Therefore we write the block Hamiltonian as

$$H_b = \epsilon c_2 - K[\bar{\alpha}_1 \alpha_2 + \bar{\alpha}_2 \alpha_1] , \tag{17}$$

where

$$c = \begin{pmatrix} 0 & 0 \\ 0 & 1 \end{pmatrix}, \qquad \alpha = \begin{pmatrix} 0 & 1 \\ 0 & i\tau \end{pmatrix}, \qquad \bar{\alpha} = \begin{pmatrix} 0 & 0 \\ 1 & i\tau \end{pmatrix}.$$

Diagonalizing eq. (17) we obtain, apart from the zero eigenvalue which corresponds to $|0\rangle_b = |\uparrow\uparrow\rangle$, the cubic equation

$$\epsilon_b^3 - 2(\epsilon + K\tau^2)\,\epsilon_b^2 + [(\epsilon + K\tau^2)^2 - K^2(1-\tau^2)^2]\,\epsilon_b + \epsilon K^2(1-\tau^2) = 0\,, \quad (18)$$

its lowest root being of interest to us. The normalized eigenvector is

$$|1\rangle_b = \frac{A_1|\downarrow\uparrow\rangle + A_2|\uparrow\downarrow\rangle + A_3|\downarrow\downarrow\rangle}{|A|}\,, \quad (19)$$

where

$$A_1 = [\epsilon_b - (\epsilon + K\tau^2)^2] + K^2\tau^2(1-\tau^2)\,,$$

$$A_2 = -K[\epsilon_b - (\epsilon + K\tau^2)]\,, \qquad A_3 = -iK\tau[\epsilon_b - (\epsilon + K)]\,,$$

$$|A| = \Big(\sum_{e=1}^{3} A_e^2\Big)^{1/2}\,.$$

The arrows in the kets indicate in an obvious way the spin up or down states of each site. We remind that in the corresponding bras one must not conjugate the complex coefficients.

The new energy gap is defined as

$$\epsilon' = {}_b\langle 1|(H_b + \epsilon c_1)\,|1\rangle_b = \epsilon_b + \frac{A_1^2 + A_3^2}{|A|^2}\,. \quad (20)$$

To evaluate the new coupling constant we must calculate the matrix elements of the field operators in the basis $|0\rangle_b$, $|1\rangle_b$ giving

$$\bar{\alpha}_1 = \begin{pmatrix} 0 & 0 \\ \dfrac{A_1}{|A|} & \dfrac{i\tau(A_1^2 + A_3^2) + A_2A_3}{|A|^2} \end{pmatrix} \quad (21)$$

and the transposed matrix for α_1. For the matrix elements of the field in site 2 one interchanges 1 and 2. In this way we obtain

$$K' = K\frac{A_1A_2}{|A|^2}\,, \quad (22)$$

and τ' as the ratio of the diagonal to non-diagonal elements of the matrix in eq. (21).

One must note that for $|\tau| \neq 1$ the value of τ' extracted with site 2 is slightly different from that obtained with site 1, showing that the form of the Hamiltonian is not exactly conserved through the renormalization group procedure. Since the difference between the two values of τ' disappears for $|\tau| \to 1$ * and the values of

* e.g., for $\tau = 0.5$ and $\epsilon/K = 1$, $\tau'_1 = 0.56$ and $\tau'_2 = 0.64$, whereas for $\tau = 0.9$ and the same ϵ/K, $\tau'_1 = 0.92$ and $\tau'_2 = 0.96$.

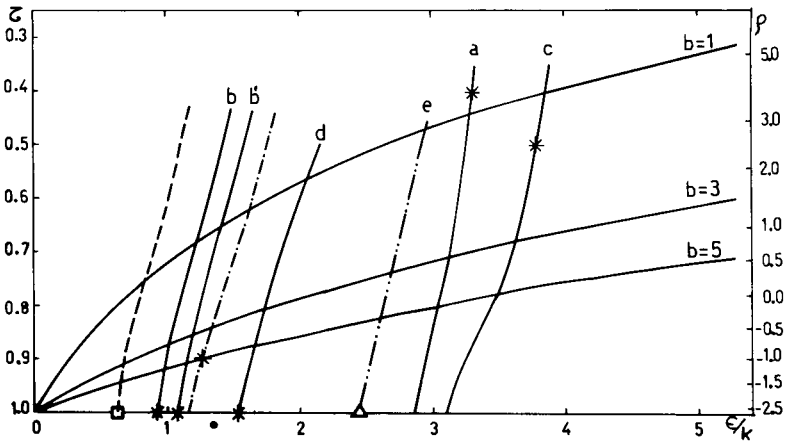

Fig. 2. Critical curves and intercepts (eq. (16)). Dashed curve: $D = 1$ critical curve in τ, ϵ/K plane for one-site, one-link blocks; dot-dashed curve: $D = 1$ critical curve for two-site, one-link blocks; □: $D = 1$ critical temperature from ref. [5]. $D = 2$ critical curves for different models are shown together with the extrapolation (two-dot-dashed curve) of the critical temperature Δ. Fixed points are denoted by *. Physical lines for constant b are parametrized by the values of ρ given on the right.

interest for the realistic parameters are near this point, we have taken the average of τ_1' and τ_2' in each step.

The numerical calculation gives a curve of critical values of $T = \epsilon/K$ as function of τ as shown in fig. 2. It must be remarked that even though the values of τ are actually negative, only $|\tau|$ is relevant for the renormalization group procedure, eqs. (20)–(22).

It is interesting to note that for $|\tau| = 1$ the lowest eigenvalue of eq. (18) is exactly zero and

$$\epsilon' = \epsilon \frac{T(T+2)}{(T+1)^2}, \qquad K' = \frac{K}{T+1}, \tag{23}$$

i.e., $|\tau'| = 1$. This is at variance with the method of keeping both site energies in the block [3] where, starting from $|\tau| = 1$, it turns out that $|\tau'| \neq 1$, being necessary to enlarge the number of parameters. From eq. (23) it is clear that $T' = T(T+2)/(T+1)$ so that the non-trivial fixed point is $T_c = (-1 + \sqrt{5})/2 = 0.618$. This value is in remarkable agreement with the one obtained from the high-temperature expansion [5] which is $T_c = 0.606$.

3.1.2. $D = 2$.

The easiest way to consider the realistic two-dimensional case is to take two-site blocks and couple them alternatively in either direction [3]. Since in the x direction there is only one link between blocks whereas in the y direction there are two links,

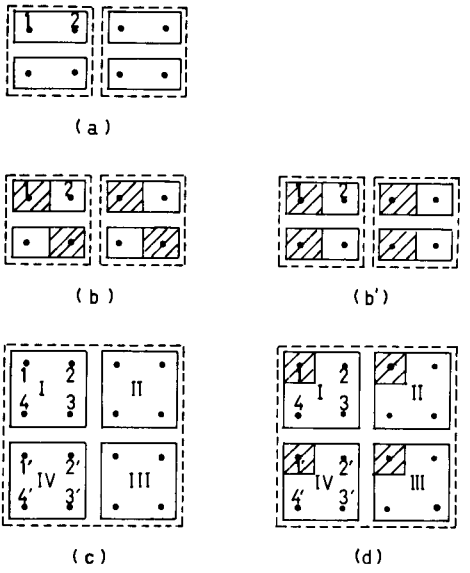

Fig. 3. Different block prescriptions. Shaded squares denote omission of site energy.

the average prescription is to multiply the recursion relation defining K' by $\sqrt{2}$ (see fig. 3a). When the block Hamiltonian includes both energy sites this constitutes model (a) and for $|\tau| = 1$ the critical ratio of parameters turns out to be [3] $T_c = 2.87$.

When one omits one energy site in the block Hamiltonian, the above method defines model (b). Since now the two sites in each cell are not equivalent, we may consider the chains as in fig. 3b, so that all the links are of the same mixed type, and again a factor $\sqrt{2}$ must be introduced on the right-hand side of the expression for K' in eq. (23). Alternatively, if the chains are thought as in fig. 3b', one has one mixed link in the x direction and two direct-type links in the y direction. This is taken into account by replacing eq. (22) by $K' = K\sqrt{A_1 A_2 (A_1^2 + A_2^2)}/|\boldsymbol{A}|^2$. The outcome is that for $|\tau| = 1$ $T_c = 0.93$ or $T_c = 1.08$ for model (b) or (b') respectively, and for different values of τ the critical curves are shown in fig. 2. Using the high-temperature expansion [5] the result for $|\tau| = 1$ was $T_c = 2.43$. The impression is, therefore, that the method of coupling two-site blocks in alternate directions gives too low values of T_c when one starts from the correct value for $D = 1$.

To avoid this procedure we may consider cells of four sites. We face again two possibilities [10], either to include the four site energies in the block Hamiltonian (model (c)), or to include only three of them (model (d)). These blocks are described in figs. 3c, d, respectively. Both possibilities respect the isotropy of the coupling between cells. It is interesting to remark that this isotropy would also be respected if we omitted the energy of both sites 1 and 3, which would give the correct ratio of

site and link terms in one block. However, diagonalizing the block Hamiltonian for $|\tau| = 1$ and then adding the expectation values of the energies of sites 1 and 3 in the two lowest levels, these states remain degenerate, it being impossible to define ϵ' and continue the renormalization group procedure. We are therefore restricted to the two abovementioned possibilities.

In both cases we must write the 16×16 matrix of the block Hamiltonian. The inclusion or omission of the site-1 energy is denoted by a variable x which takes the values 1 and 0, respectively. Through the diagonalization of the block Hamiltonian we get, apart from the vacuum which corresponds to the four "spins up" state, a lowest energy, ϵ_b, state of the form

$$|1\rangle_b = b_2\begin{pmatrix}\downarrow\uparrow\\ \uparrow\downarrow\end{pmatrix} + b_3\begin{pmatrix}\uparrow\downarrow\\ \downarrow\uparrow\end{pmatrix} + b_4\begin{pmatrix}\downarrow\downarrow\\ \downarrow\downarrow\end{pmatrix} + b_5\begin{pmatrix}\downarrow\uparrow\\ \uparrow\uparrow\end{pmatrix} + b_6\begin{pmatrix}\uparrow\downarrow\\ \uparrow\uparrow\end{pmatrix} + b_7\begin{pmatrix}\uparrow\uparrow\\ \uparrow\downarrow\end{pmatrix}$$
$$+ b_8\begin{pmatrix}\uparrow\uparrow\\ \downarrow\uparrow\end{pmatrix} + b_9\begin{pmatrix}\downarrow\downarrow\\ \uparrow\uparrow\end{pmatrix} + b_{10}\begin{pmatrix}\uparrow\downarrow\\ \uparrow\downarrow\end{pmatrix} + b_{11}\begin{pmatrix}\uparrow\uparrow\\ \downarrow\downarrow\end{pmatrix} + b_{12}\begin{pmatrix}\downarrow\uparrow\\ \downarrow\uparrow\end{pmatrix} + b_{13}\begin{pmatrix}\downarrow\downarrow\\ \uparrow\downarrow\end{pmatrix}$$
$$+ b_{14}\begin{pmatrix}\uparrow\downarrow\\ \downarrow\downarrow\end{pmatrix} + b_{15}\begin{pmatrix}\downarrow\uparrow\\ \downarrow\downarrow\end{pmatrix} + b_{16}\begin{pmatrix}\downarrow\downarrow\\ \downarrow\uparrow\end{pmatrix}. \tag{24}$$

When $x = 1$ the cell energy gap will be $\epsilon' = \epsilon_b$ whereas for $x = 0$

$$\epsilon' = \epsilon_b + \epsilon(b_2^2 + b_4^2 + b_5^2 + b_9^2 + b_{12}^2 + b_{13}^2 + b_{15}^2 + b_{16}^2)\,. \tag{25}$$

The new τ is obviously defined by

$$i\tau' = \frac{{}_b\langle 1|\alpha|1\rangle_b}{{}_b\langle 0|\alpha|1\rangle_b}\,. \tag{26}$$

For site 1, e.g., we have

$${}_b\langle 1|\alpha_1|1\rangle_b = i\tau(b_2^2 + b_4^2 + b_5^2 + b_9^2 + b_{12}^2 + b_{13}^2 + b_{15}^2 + b_{16}^2)$$
$$+ b_2b_7 + b_4b_{14} + b_9b_6 + b_{12}b_8 + b_{13}b_{10} + b_{15}b_{11} + b_{16}b_3$$
$$= {}_b\langle 1|\alpha_1|1\rangle_b\,, \tag{27}$$

and

$${}_b\langle 0|\alpha_1|1\rangle_b = b_5 = {}_b\langle 1|\bar{\alpha}_1|0\rangle_b\,. \tag{28}$$

The interaction between cells I and IV is

$$K(\bar{\alpha}_{1'}\alpha_4 + \bar{\alpha}_{2'}\alpha_3 + \bar{\alpha}_4\alpha_{1'} + \bar{\alpha}_3\alpha_{2'})\,,$$

as one can see from figs. 3c, d. Note that taking the coupling between cells I and II, the same expression appears because of the symmetry $2 \leftrightarrow 4$ in each block. Thus, the new coupling constant will be

$$K' = K(b_5b_8 + b_6b_7)\,. \tag{29}$$

The eigenvalue ϵ_b and eigenvector $|1\rangle_b$ have been obtained numerically and the

Table 3
Critical temperature and critical intercept for $D = 2$

$D = 2$ model	$T_c(\tau = 1)$	α_c		
		$b = 1\ \mathrm{GeV}^{-1}$	$b = 3\ \mathrm{GeV}^{-1}$	$b = 5\ \mathrm{GeV}^{-1}$
(a)	2.87	1.21	1.07	1.05
(b)	0.93	1.80	1.18	1.10
(b')	1.08	1.74	1.16	1.09
(c)	3.10	1.07	1.05	1.04
(d)	1.54	1.55	1.13	1.08
(a')	2.87	1.19	1.08	1.06
(e) extrapolation of ref. [5]	2.43	1.30	1.08	1.06

Critical temperature $T_c = \epsilon/K$ for $\tau = 1$ and pomeron critical intercept are given for different block-spin prescriptions and values of intersite spacing b. Dots denote sites. Open circles indicate omitted energy sites according to refs. [9] and [10]. Parentheses show sites forming a block. Lines between sites correspond to the intersite interaction including diagonal terms of $\nabla\bar{\psi} \cdot \nabla\psi$ as in eq. (30).

critical curves for both models (c) and (d) are shown in fig. 2. For model (c) the value of τ', eq. (26), is obviously the same for all sites. For model (d) this is only true for $|\tau| = 1$ when $|\tau'| = 1$ for all sites. However, the variations in τ' calculated for different sites are slight (e.g., for $|\tau| = 0.8$ and $\epsilon/K = 1.5$, $\tau'_1 = 0.89$, $\tau'_2 = \tau'_4 = 1.01$, $\tau'_3 = 1.05$) so that we have taken the average to preserve the form of the Hamiltonian. We remark that for $|\tau| = 1$ the eigenvalue ϵ_b is again zero for model (d), confirming that when the omission trick preserves exactly the form of the Hamiltonian, the two lowest states obtained by diagonalization of the block Hamiltonian are degenerate.

Using the relation between ρ and α_0, r_0, α' and b, $\alpha_0 = 1 - r_0\rho/2b + 4\alpha'/b^2$, and the single-site results for λ_1, $\langle 0|\psi|1\rangle$ and $\langle 1|\psi|1\rangle$ contained in table 1, one is able to obtain the critical value of the pomeron intercept α_c for the different methods. This corresponds to the intersection of the critical curves with the physical one which gives ϵ/K and τ for each ρ. We have kept fixed the values of $r_0 = 0.5\ \mathrm{GeV}^{-1}$ and $\alpha' = 0.25\ \mathrm{GeV}^{-2}$. Several values of b have been considered: since the cutoff in momentum transfer is $t \simeq \pi^2/b^2$, the realistic value of b should be in the range $1-5\ \mathrm{GeV}^{-1}$. The numerical values for α_c, together with the critical $T_c = (\epsilon/K)_c$ obtained for $|\tau| = 1$ (see fig. 2), are shown in table 3. For $D = 2$ it appears that the 4-site blocks without omission give too high a T_c, but with omission this value is too low.

Since from fig. 2 one sees that all the critical curves are approximately parallel, we have drawn a line with average slope extrapolating the high-temperature expansion point for $\tau = 1$, which we have also denoted as model (e) in table 3.

3.2. Inclusion of the diagonal part of $\nabla\bar{\psi} \cdot \nabla\psi$ in the intersite interaction

We shall consider the variation in α_c due to this modification using the two-site blocks for $D = 2$ in the version of model (a). The block Hamiltonian must be written as

$$H_b = \epsilon(c_1 + c_2) + L(c_1 + c_2) - K(\bar{\alpha}_1\alpha_2 + \bar{\alpha}_2\alpha_1) , \tag{30}$$

where the energy gap ϵ is determined by the single-site problem equation, (3), with $\rho = 2\Delta_0/r$. K, $\bar{\alpha}$ and α are defined as in eqs. (16) and (17), and the new coupling constant is $L = 4\alpha'\langle 1|\bar{\psi}\psi|1\rangle/b^2$.

Though the second term of eq. (30) may be obviously added to the first term, its inclusion in the intersite interaction might be sensible since the term $\nabla\bar{\psi} \cdot \nabla\psi$ could be smaller than its non-diagonal part.

Diagonalizing eq. (30) one gets as new energy gap

$$\epsilon' = \tfrac{1}{2}\{3(\epsilon + L) + 2K\tau^2 - K - [(\epsilon + L)^2 + 4(\epsilon + L)K\tau^2 + 2(\epsilon + L)K + (2K\tau^2 - K)^2]^{1/2}\} . \tag{31}$$

Coupling two horizontal cells one defines again

$$K' = A^2K , \qquad \tau' = \frac{1}{A}[(A^2 - B^2)\tau + AB] , \tag{32}$$

where

$$A^2 = \frac{K^2\tau^2}{2K^2\tau^2 - (K + \epsilon' - \epsilon - L)^2} , \qquad B = \frac{(K + \epsilon' - \epsilon - L)A}{K\tau} ,$$

are the coefficients of the first excited cell state $|1\rangle_b = A|\uparrow\downarrow\rangle + A|\downarrow\uparrow\rangle + iB|\downarrow\downarrow\rangle$. Expressions (31) and (32) are analogous to the ones of ref. [3] with $\epsilon + L$ replacing ϵ. The new coupling constant for cells, L', is obtained by building the matrix of c in the subspace of states $|0\rangle_b$ and $|1\rangle_b$. In this way

$$L' = L(A^2 - B^2) . \tag{33}$$

Eqs. (31)–(33) constitute our new recursion relations since the two-cell Hamiltonian keeps the same form as the two-site Hamiltonian, eq. (30). Since coupling two cells in the vertical direction causes two intersite interactions to appear, we take an average, inserting $\sqrt{2}$ in the right-hand side of the definition of K', eq. (32). This constitutes our model (a'), its blocks being analogous to those of fig. 3a.

As we have seen before in table 1, the matrix element $\langle 1|\bar{\psi}\psi|1\rangle$ is very accurately saturated by inserting $|0\rangle$ and $|1\rangle$ as intermediate states. With this approximation

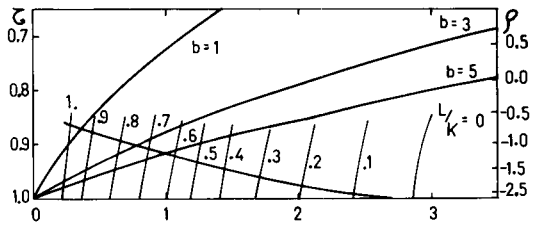

Fig. 4. Inclusion of diagonal terms of $\nabla\bar{\psi} \cdot \nabla\psi$ in the intersite interaction (eq. (30)). Sections of the critical surface with constant L/K planes are shown. The consistency curve comes from the physical constraint $L/K = 4(1 - \tau^2)$. Critical intercepts are obtained from the intersection of the consistency curve with physical lines for each value of b.

$L \simeq 4(1 - \tau^2) K$ so that if $|\tau| = 1$, L vanishes and our model (a') coincides with model (a) of ref. [3]; but starting from the realistic $|\tau| \neq 1$, three relevant parameters ϵ/K, τ and L/K must be considered, so that instead of a critical curve, a critical surface appears. Its interactions with constant L/K planes are shown in fig. 4. The consistency curve for physical configurations is obtained by joining points where $L/K = 4(1 - \tau^2)$ holds. The intersection of this consistency curve with the physical lines for each fixed b allows one to calculate the corresponding critical intercepts according to $\alpha_0 = 1 - r_0\rho/2b$.

The values shown in table 3 indicate that the agreement with model (a) is quite good. The slight differences may be a consequence of the more elaborate way of obtaining α_c in model (a') due to the additional parameters. It seems, therefore, that both methods are equivalent. Though in model (a') the intersite interaction is smaller, the energy gap is also smaller, compensating the previous effect.

4. Conclusions

Our aim has been to obtain the critical intercept of the pomeron starting from realistic values of the RFT parameters.

We have been able to calculate accurately the single-site properties of the RFT on a lattice. From these it is clear that the two-level approximation may introduce a non-negligible error in the renormalization group procedure even though it has been shown [7] that the inclusion of a third level only slightly changes the lowest lying excited energy in the first step.

Regarding the intersite interaction two problems have been examined: the procedure of building block-spins and the definition of the interaction term.

For $D = 1$ it appears that taking the one-site one-link contributions [9] as the block Hamiltonian, remarkable agreement is obtained between the critical $T = \epsilon/K$ for the limiting case $|\tau| = 1$ and the high-temperature expansion [5]. On the contrary, the normal two-site procedure [3] gave too high a T_c.

For $D = 2$, coupling two-site cells alternatively in the horizontal and vertical directions and using the omission trick, or using four-site cells omitting the energy of one site, give values of T_c too low compared to the high-temperature expansion. Conversely, too high a value of T_c results from a normal four-site block procedure. A slightly better result appears using the alternative coupling of normal two-site cells [3], probably because of compensating effects. The critical intercept α_c obtained in this way coincides with the one of ref. [7] for $b = 1$ but disagrees for $b = 3$ due to the fact that in ref. [7] the phase transition had been reached only for $b = 1$.

Looking at the possibility of including the diagonal part of $\nabla\bar{\psi} \cdot \nabla\psi$ in the intersite interaction, which might be sensible since the fields are not expected to vary too much in the lowest energy states, the results for α_c do not change. This method cannot be considered as better than the previous one because the energy gap decreases together with the intersite interaction.

In the realistic range of $1 < b < 5\ \mathrm{GeV}^{-1}$ the models which predict T_c around the high-temperature expansion value give $\alpha_c \gtrsim 1.05$. Therefore, a critical pomeron theory may be in agreement [6] with experimental data.

We wish to thank John Cardy, whose visit has been supported by OAS Multinational Program of Physics, for interesting discussions and valuable comments.

Note added

After the completion of this paper we received a preprint [14] in which the single-site energies and the matrix elements $\langle 0|\psi|n\rangle$ have been accurately computed by a method different to our own. The numerical values of λ_1 quoted by these authors coincide with ours up to the last significant figure shown in table 1. Regarding the values of λ_2 and $\langle 0|\psi|n\rangle$, which are given in the figures of ref. [14], the agreement with our results is also excellent.

References

[1] H.D.I. Abarbanel, J.B. Bronzan, R.L. Sugar and A.R. White, Phys. Reports 21 (1975) 119; M. Moshe, Phys. Reports 37 (1978) 255.
[2] D. Amati, M. Ciafaloni, M. Le Bellac and G. Marchesini, Nucl. Phys. B112 (1976) 107.
[3] J.L. Cardy, Nucl. Phys. B115 (1976) 141.
[4] R.C. Brower, M.A. Furman and K. Subbarao, Phys. Rev. D15 (1977) 1756.
[5] R.C. Brower, M.A. Furman and M. Moshe, CERN preprint TH. 2458 (1978).
[6] A. Della Selva, L. Masperi, V. Roberto amd A. Ungkitchanukit, Nucl. Phys. B127 (1977) 413;
L. Masperi, Phys. Lett. 73B (1978) 335.
[7] L. Masperi, V. Roberto and A. Ungkitchanukit, Nucl. Phys. 140 (1978) 301.
[8] R. Jengo, Nucl. Phys. B108 (1976) 447.
[9] A. Fernández Pacheco, Stanford preprint SLAC-PUB-2099 (1978).
[10] A. Fernández Pacheco, Stanford preprint SLAC-PUB-2117 (1978).

[11] M; Ciafaloni, M. Le Bellac and G.C. Rossi, Nucl. Phys. 130 (1977) 388.
[12] J.R. Fulco and L. Masperi, Phys. Rev. D19 (1979) 690.
[13] E. Fradkin and L. Susskind, Phys. Rev. D17 (1978) 2637.
[14] R. Blankenbecler and R.L. Sugar, Stanford preprint SLAC-PUB-2251 (1979).